UDC 539.3

OPTIMIZATION OF A VIBRO-IMPACT DAMPER DESIGN USING MATLAB TOOLS

P.P. Lizunov

O.S. Pogorelova

T.G. Postnikova

Kyiv National University of Construction and Architecture
31, Povitryanykh Syl ave., Kyiv, Ukraine, 03680

DOI: 10.32347/2410-2547.2024.112.3-18

The paper studies the possibility of optimizing the parameters of a nonlinear energy sink (NES) using standard software. It is shown that optimization procedures do not give an unambiguous result, since many sets of damper parametersprovide the best mitigation of the primary structure vibrations. The dynamicsof the system with each set of parametersmust be carefully tested and analyzed. It exhibits various interesting modes, namely 1:1 resonance, 2:1 resonance, and amplitude modulated signal .

Keywords:optimization, damper, parameter set, vibro-impact, nonlinear energy sink.

1. Introduction

Vibro-impact dampers are devices for passive suppression of unwanted vibrations. They are designed to reduce vibration of the main (primary) structure. During the oscillatory motion of a system consisting of a main structure and a damper coupled with it, the damper takes up some of the main structure energy. This is the so-called Targeted Energy Transfer (TET) [1-3]. By taking on some of the main structure energy, the damper reduces the amplitudes and velocities of its vibrations. This reduction is due to the significant system nonlinearity. Nonlinear dampers were proposed as an evolution of devices known as Tuned Mass Dampers (TMD) [4,5], which were linearly coupled to the main structure. The nonlinear dampers have been called Nonlinear Energy Sinks (NESs) [6-8]. Their nonlinearity is of a different nature, ranging from cubic springs to impacts. The different NESs types with different nonlinearity have been proposed and studied for two decades [9-12]. In the newest survey [13], the authors show an increase in the number of publications on NES from the Web of science database from 2009 to 2023. This review contains an extensive bibliography.

A vibro-impact NES (VI NES) is one of the NES types, widely discussed in the scientific literature [1, 14, 16]. Selecting the optimal damper design is one of the main challenges in damper application. In their works, the authors have proposed different algorithms to optimize the damper parameters [6,16-18]. These algorithms are oriented to the specific problems considered in their research. However, no optimization procedure provides or can provide an unambiguous result. This is due to the presence of a large number of damper parameter sets that provide maximum mitigation of the main structure vibrations. Consideration of synergistic effect is also important. It would be desirable to optimize as many parameters as possible simultaneously. The sequence of actions of the optimization procedure itself is also ambiguous. This paper shows the possibility of using standard MATLAB tools to optimize the vibro-impact damper parameters. We show how using different combinations of these tools can produce different parameter sets. Naturally, each damper design demonstrates different dynamics of a strongly nonlinear discontinuous 2-DOF (two degrees of freedom) vibro-impact system consisting of a main structure and a vibro-impact damper coupled with it. The actual dynamics must be analyzed to evaluate the feasibility of the application the damper with the selected design. The work shows the changing of the oscillatory regimes for different damper designs when the exciting force frequency changes. In particular, we observed periodic regimes of different types, namely 1:1 resonance, 2:1 resonance and strongly modulated response.

The choice of the impact rule, that is, the simulation of the repeated impacts, is very important for any vibro-impact system. More often the impacts are considered instantaneous. Impact accounting is realized by recording the velocity jump at the impact moment. This velocity jump is captured by Newtonian coefficient of restitution. In other impact models, the contact force models its action. The contact force can be described either linearly or nonlinearly. The problem of simulation the rigid (hard) and soft

ISSN 2410-2547
Опір матеріалів і теорія споруд/Strength of Materials and Theory of Structures. 2024. № 112

impacts is discussed in many works, both recent [19-22] and earlier [23, 24]. The paper [21] proposes a finite contact duration model for a VI NES. After examining this problem in our previous works [25, 26], we simulate an impact by Hertz's nonlinear contact force according to his quasi-static contact theory [27, 28].

Thus, the goals of this paper are as follows:

- show how to select an optimal VI NES design using standard MATLAB tools;
- show the manifold of possible sets of optimal damper parameters;
- show the analysis of the system dynamics for different damper designs.

2. Model description and governing equations

The model under consideration is a mechanical two-mass two-degree-of-freedom (2-DOF) vibro-impact system, which was considered in our previous papers [29-31]. Therefore, we give a brief description of it. A heavy primary structure (PS) of m_1 mass is attached to a fixed wall by a linear elastic spring with a stiffness k_1 and a damper with a damping coefficient c_1. It is coupled with a lightweight vibro-impact damper of m_2 mass by linear spring k_2 and a damper c_2; $m_2 << m_1$. During the system oscillatory movement, a vibro-impact damper repeatedly hits an obstacle rigidly connected to the PS. The scheme presented in Fig. 1 corresponds to the conceptual scheme of the single-sided vibro-impact NES – SSVI NES [4, 8, 32]. However, as we have shown in our previous works and in this paper, the damper hits not only the obstacle, but also the primary structure directly. Then it could be called a double-sided VI NES (DSVI NES). That's why we just write VI NES.

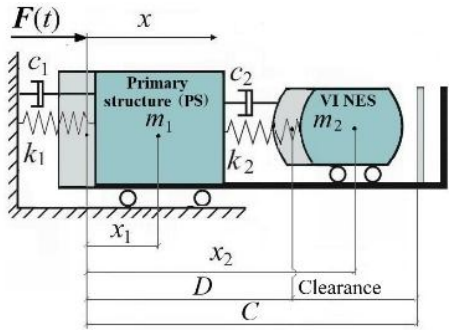

Fig. 1. Calculation scheme of VI NES

All designations and distance specifications are shown in Fig. 1. Let's emphasize only the notion of clearance. Since both bodies perform translational motion, we consider their movement as the movement of the mass centers. Therefore, the clearance is the distance between the mass center of the damper in its initial position and the obstacle also in the initial position; it is defined as (C - D).

We believe that primary structure parameters are set in advance and are not subject to optimization. In this article, we will not vary their values: m_1=1000 kg, k_1=3.95·10^{4}N/m, c_1=452 N·s/m, $E_1 = E_2$ =2.1·10^{11} N/m^2, $\nu_1 = \nu_2$ =0.3.

In this paper, we study this system under action of harmonic force $F(t) = P\cos(\omega t + \varphi_0)$. P = 800 N, ω = 6.3 rad/s. Its period is $T = 2\pi/\omega$.

The problem of impact simulation is very important in vibro-impact systems. In all our works, we simulate an impact by nonlinear contact interactive force in accordance with Hertz's quasi-static contact theory [27, 28]. According to this theory, the impact has a finite duration; the local deformations of colliding surfaces in the contact zone are allowed. A contact force acting only during an impact simulates the impact action:

$$F_{con}(z) = K[z(t)]^{3/2}. \quad (1)$$

Here z is the colliding bodies rapprochement upon impact. We consider the damper impacts on both the PS directly and the obstacle.

The impacts can occur when:

$x_1 \geq x_2$ that is, $x_1 - x_2 \geq 0$ (on PS);

$x_2 \geq x_1 + C$ that is, $x_2 - x_1 - C \geq 0$ (on obstacle).

Then for these impacts the bodies rapprochements are

$z_1 = x_1 - x_2$ (for direct impacts on PS);

$z_2 = x_2 - x_1 - C$ (for impacts on an obstacle).

The coefficient K characterizes the mechanical and geometrical properties of colliding surfaces. Therefore, it differs for damper impacts on the PS and the obstacle:

When impacting the PS	**When impacting the obstacle**
$K_1 = \frac{4}{3}\frac{q_1}{(\delta_1+\delta_2)\sqrt{A_1+B_1}},$	$K_2 = \frac{4}{3}\frac{q_2}{(\delta_3+\delta_4)\sqrt{A_2+B_2}},$
$\delta_1 = \frac{1-\nu_1^2}{E_1\pi},\ \delta_2 = \frac{1-\nu_2^2}{E_2\pi}.$	$\delta_3 = \frac{1-\nu_3^2}{E_3\pi},\ \delta_4 = \frac{1-\nu_4^2}{E_4\pi}.$

(2)

Here the Young's moduli of elasticity for all surfaces E_1, E_2, E_3, E_4 and Poisson's ratios $\nu_1, \nu_2, \nu_3, \nu_4$ are included into the characteristics of colliding surfaces. Their geometric characteristics are also included in the consideration; they are $A_1, A_2, B_1, B_2, q_1, q_2$. We assume thatthe damper surfaces, both left and right, are spherical with large radii R_1 and R_2, and the contact surfaces of the primary structure and the obstacle are flat. Then $A_1 = B_1 = 1/2R_1$, $A_2 = B_2 = 1/2R_2$ we set $A_1 = A_2 = B_1 = B_2 = 0.5\,\mathrm{m}^{-1}$, $q_1 = q_2 = 0.319$ as in the collision of a plane and a sphere. We included elastic moduliin the list of optimized parameters and obtained the system responses to their changes. This made it possible to analyze the effect of changing the mechanical characteristics of colliding surfaces in more detail than the more prevalent consideration of the Newtonian restitution coefficient [23].

Then the motion equations for this system are as follows:

$$m_1\ddot{x}_1 + c_1\dot{x}_1 + k_1x_1 - c_2(\dot{x}_2 - \dot{x}_1) - k_2(x_2 - x_1 - D) = F(t) - H(z_1)F_{con}(z_1) + H(z_2)F_{con}(z_2),$$
$$m_2\ddot{x}_2 + c_2(\dot{x}_2 - \dot{x}_1) + k_2(x_2 - x_1 - D) = H(z_1)F_{con}(z_1) - H(z_2)F_{con}(z_2). \quad (3)$$

The initial conditions are

$$\text{at } t = 0, \text{ we have } x_1(0) = 0,\ x_2(0) = D,\ \dot{x}_1(0) = \dot{x}_2(0) = 0,\ \varphi_0 = 0. \quad (4)$$

The Heaviside step function $H(z) = \begin{cases} 1, & z \ge 0 \\ 0, & z < 0 \end{cases}$ "activates" the contact force.

The vibro-impact system under consideration is strongly nonlinear discontinuous one. The set of the motion equations Eq.3 is the stiff set of the Ordinary Differential Equations (ODE). Its integration requires not only changing the size of the integration step, but also making it extremely small. The MATLAB platform offers several solvers designed for stiff ODEs, known as *stiff* solvers. We use one of them, namely *ode23s* solver. The variable-step solver *ode23s* adjusts the integration step size. This allows us to determine with sufficient accuracy the instant when the Heaviside function becomes equal to unity, that is, in our problem the bodies collision begins.

The total energy of the primary structure, the reduction of which is the aim of the damper parameters optimization, is calculated using the well-known formula:

$$E_{1total}(t) = E_{1kinetic}(t) + E_{1poten}(t) = \frac{m_1\dot{x}_1(t)^2 + k_1x_1(t)^2}{2}. \quad (5)$$

3. Optimization procedures

Optimization procedures are performed to find the optimal VI NES design. A damper with optimal parameters should best mitigate the vibrations of the primary structure (PS).

First of all, we want to emphasize that "there is no exact methodto simplify the design of the multiparameter nonlinear energy sinks" [13].

Optimization procedures do not provide an unambiguous result. It is noted in [6] that there are many sets of parameter values that provide the objective function minimum. "The nonlinear stiffness properties have significant influence on control effectiveness, and they can be implemented in numerous scenarios with plenty of configuration parameters". We have carried out the optimization procedures using the tools of standard MATLAB software.

Setting the objective function and its parameters plays a crucial role in the optimization process. Naturally, some of these parameters are precisely the ones to be optimized.

We have chosen the maximum total energy of the primary structure as the objective function. The PS total energy is calculated by formula (5).

ISSN 2410-2547
Опір матеріалів і теорія споруд/Strength of Materials and Theory of Structures. 2024. № 112

3.1. Finding local minima

We have found the optimal design of VI NES in our previous articles [29, 31, 33]. We have used the programs of the MATLAB platform *fminsearch* and *fmincon*, which allow us to find local minima of the objective function. We have optimized the damper mass m_2, stiffness k_2, and damping coefficient c_2 as recommended in the scientific literature. We then have optimized the damper layout, i.e. the initial distance D between VI NES and the primary structureand the distance C to the obstacle rigidly connected to it. The difference (C -D) determines the clearance. We have also optimized the elastic moduli E_2 and E_4, which characterize the mechanical properties of the colliding surfaces. The multiple parameters optimization has shown the amazing synergistic effect. The results obtained are as follows. We have looked at the two best options ***V1*** and ***V2*** with significantly different parameters.

V1: m_2=39.67 kg, k_2 = 1550.7 N/m, c_2=643.6 N·s/m, C=0.124 m,
D = 0.1002 m, E_2=2.21·10^7 N/m^2, E_4=2.05·10^7 N/m^2, v_2=v_4=0.4.

V2: m_2=62.02 kg, k_2 = 198.24 N/m, c_2=538.8 N·s/m, C=0.0498 m,
D = 0.000001 m, E_2=2.21·10^7 N/m^2, E_4=2.05·10^7 N/m^2, v_2=v_4=0.4.

Fig. 2 shows the dependence of the maximum total energy of the primary structure coupled to a VI NESs of these two options on the exciting force frequency.

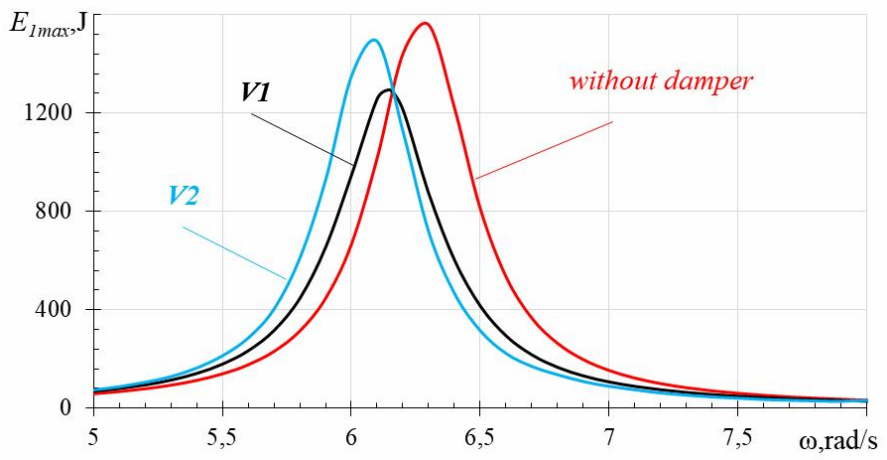

Fig.2. The dependence of the maximum total energy of the PScoupled to different VI NES of variants***V1***, ***V2*** on the exciting force frequency

The lightweight damper of ***V1*** variant has a mass m_2 that is about 4% of the PS mass m_1. It reduces the resonant peak of the PS energy. It also reduces this energy over a wide range of exciting force frequencies that are larger than the resonant one. The lightweight damper of ***V2*** variant has a mass m_2 that is about 6% of the PS mass m_1. It also reduces the resonant peak of the PS energy, but to a lesser extent. But in the range of exciting force frequencies exceeding the resonant one, it reduces the total energy of the PS more strongly.

3.2. Optimization over wider parameters ranges

The optimal damper design shown in the previous section was obtained by searching for local minima. However, as we have already noted, there are many sets of parameters values that provide the objective function minimum. The MATLAB *surf* program allows you to obtain the quite wide parameters ranges with corresponding objective function values. Note that the genetic algorithm *ga* of MATLAB platform makes a random selection during its operation, and then specifies some random parameters set from these ranges. But the figures of these parameters ranges are ambiguous. They depend on the parameters values chosen for the objective function calculation. They also depend on the bounds that are set for the parameters to be optimized.

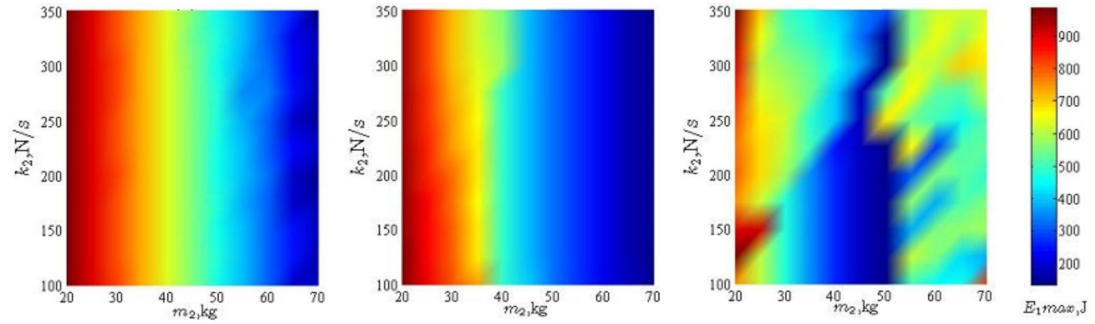

c_2 =40.7 N·s/m; D=0.05 m; C=0.06 m; E_2 =2.1·10^{11}N/m^2; E_4 =2.1·10^{11} N/m^2; $v_2 = v_4 = 0.3$ (a)

c_2 =232 N·s/m; D=0.06 m; C=0.36 m; E_2 =2.21·10^7 N/m^2; E_4 =2.05·10^7 N/m^2; $v_2 = v_4 = 0.4$ (b)

c_2 =64 N·s/m; D=0.03 m; C=0.673 m; E_2 =2.21·10^7 N/m^2; E_4 =2.05·10^7 N/m^2; $v_2 = v_4 = 0.4$ (c)

Fig. 3. The relationship between damper parameters m_2, k_2 at different values of other parameters

The parameters of the primary structure m_1, k_1, c_1, E_1, E_3 and the exciting force P, ω do not change; they are given in Sec. 2. Fig. 3 shows the relationship between damper parameters m_2, k_2 at different values of other parameters. Color determines the objective function values, that is, the values of the maximum total energy of the primary structure.

The two left images are similar and show some independence of the PS maximum energy from the damper stiffness k_2. However, this seeming independence exists only for some values of other parameters. The right image in Fig. 3 and further analysis confirm this.

Fig. 4 shows the relationship between damper parameters m_2, c_2 at different values of other parameters.

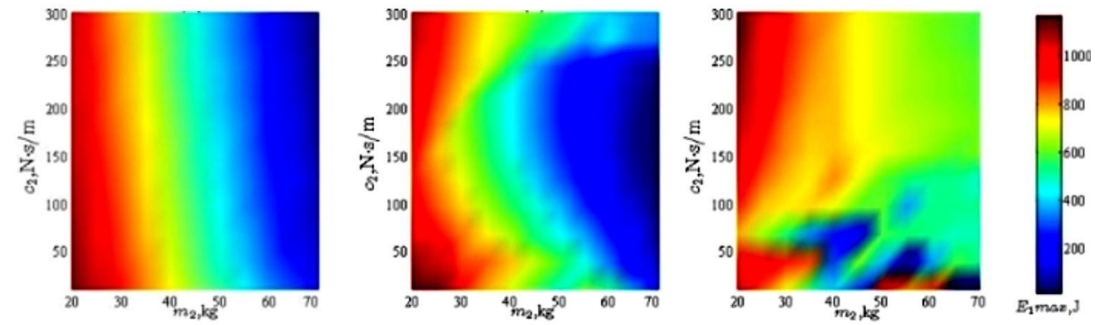

k_2 = 1500 N/m; D=0.05 m; C =0.06 m; E_2 =2.1·10^{11} N/m^2; E_4 =2.1·10^{11} N/m^2; $v_2 = v_4 = 0.3$ (a)

k_2 = 215 N/m; D=0.06 m; C=0.36 m; E_2 =2.21·10^7 N/m^2; E_4 =2.05·10^7 N/m^2; $v_2 = v_4 = 0.4$ (b)

k_2 = 215 N/m; D=0.03 m; C=0.673 m; E_2 =2.21·10^7 N/m^2; E_4 =2.05·10^7 N/m^2; $v_2 = v_4 = 0.4$ (c)

Fig. 4. The relationships between damper parameters m_2, c_2 at different values of other parameters

All of the images are significantly different from each other. The two left images in Fig. 3 and Fig. 4 suggest that higher mass dampers mitigate the primary structure energy more strongly. Therefore, we have chosen two mass values for further optimization and analysis. They are m_2=40 kg and m_2=60 kg.The same damper masses were chosen in the search for local minima in Sec.3.1. This means that we can compare the results of these searches. Note that in [34] the authors also separately analyze the performance of dampers with different masses.

The difference in the images in Fig. 3 and Fig. 4 at different values of other parameters emphasizes that only a complex of all the damper parameters can ensure its optimal design. Synergistic effect we

ISSN 2410-2547
Опір матеріалів і теорія споруд/Strength of Materials and Theory of Structures. 2024. № 112

observed in our previous work [29] supports this claim. Such a situation requires simultaneous, rather than sequential, optimization of all damper parameters. However, there is no software available to implement such simultaneous optimization. The MATLAB *fminsearch* and *fmincon* programs, which allow us to find minimum of the multivariable function, do not provide the satisfactory results. Therefore, we optimized the damper parameters alternately in several steps, testing the effect from each step.

4. Parameters optimization for damper with mass m_2=60 kg

4.1. Search of the optimal design

The mass of this damper is 6% of the primary structure mass. The parameters optimization is carried out using both the *surf* program and *fminsearch, fmincon* programs. The *surf* program shows the relationship between two parameters. The parameters values selected from the ranges shown can be precised using the *fminsearch, fmincon* programs, which find the local minimum of the objective function. This procedure is ambiguous and contains a sufficient amount of arbitrariness.

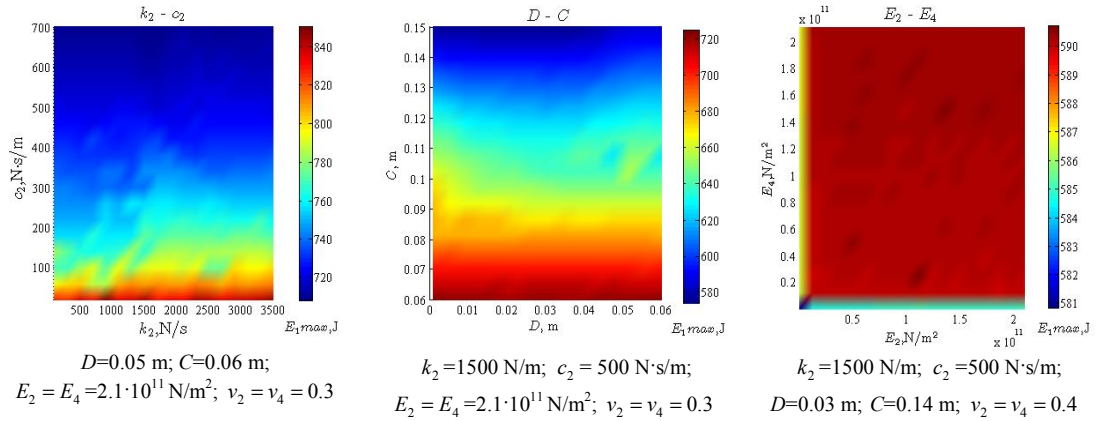

D=0.05 m; C=0.06 m;
$E_2 = E_4$ =2.1·10^{11} N/m^2; $\nu_2 = \nu_4 = 0.3$

k_2 =1500 N/m; c_2 = 500 N·s/m;
$E_2 = E_4$ =2.1·10^{11} N/m^2; $\nu_2 = \nu_4 = 0.3$

k_2 =1500 N/m; c_2 =500 N·s/m;
D=0.03 m; C=0.14 m; $\nu_2 = \nu_4 = 0.4$

k_2 = 1500 N/m; D=0.03 m;
$E_2 = E_4$ =2.0·10^7 N/m^2; $\nu_2 = \nu_4 = 0.4$

c_2 = 232 N·s/m; D=0.06 m;
$E_2 = E_4$ =2.0·10^7 N/m^2; $\nu_2 = \nu_4 = 0.4$

k_2 =215 N/m; c_2 =232 N·s/m;
D=0.06 m; C=0.36 m; $\nu_2 = \nu_4 = 0.4$

Fig. 5. The relationships between different pairs of damper parameters

After précising the parameters using the *fminsearch, fmincon* programs, we obtained the following set of damper parameters:

V3: m_2=60 kg, k_2 = 215 N/m, c_2 =232 N·s/m, C=0.36 m,
D= 0.06 m, E_2 =2.21·10^7 N/m^2, E_4 =2.05·10^7 N/m^2, $\nu_2 = \nu_4$ =0.4.

Note that setting the elastic moduli E_2, E_4, which are four orders of magnitude smaller, gives preference to a soft impact. This setting is consistent with the assignment in several articles [35, 36] to a lower restitution coefficient – 0.45 instead of 0.7.

In the next section, we show the performance of the damper with these parameters.

4.2. Dynamic behavior of the primary structure coupled to the vibro-impact damper of *V3* variant

The graph in Fig.6 shows the change in the maximum total energy of the primary structure coupled to such a damper as the exciting force frequency changes.

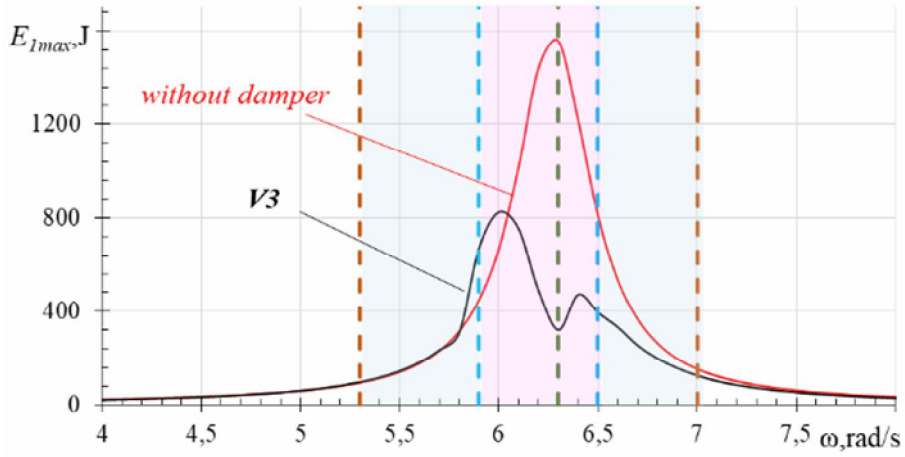

Fig. 6. Maximum total energy of the primary structure coupled to the damper of ***V3*** variant

Comparing Fig. 6 and Fig. 2, one can see how much stronger the damper of the ***V3*** variant reduces the maximum primary structure energy in the resonance region. The curve has two resonant peaks since the "PS – NES" system is a 2-DOF system. The authors [37-39] have demonstrated this phenomenon for TMD and NES. The damper parameters in ***V3*** variant are very different from the ***V2*** variant. Special attention should be paid to the large clearance (C -D)= 0.3 m. Because of this, the impacts of a vibro-impact damper on the obstacle occur only in the region of the frequencies close to the resonant one. The region of the damper impacts against both the primary structure directly and an obstacle rigidly connected to it, is quite narrow 5.9 rad/s $\le \omega \le$ 6.5 rad/s. The blue dottedvertical lines in Fig.6 mark it. It is colored pink. In the wider region, marked by brown dotted vertical lines, the damper impacts occur only on the PS directly, there are no impacts on the obstacle. This region is bounded on the left by ω =5.3 rad/s and on the right by ω =5.3 rad/s. It is colored blue. Outside this region, the T-periodic regime is realized without any impacts.Table 1 shows the regime alternation when the exciting force frequency changes. The following designations are used. We note nT, m, k periodic regime of nT periodicity with m direct damper impacts on the PS and k its impacts on an obstacle per cycle. The "Strongly Modulated Response" mode is naturally called SMR.

Periodic regimes are observed in several frequency ranges. To the left of the resonance at 5.4 rad/s $\le \omega \le$ 5.8 rad/s the 2T,1,0 mode occurs. Near resonance, the T,1,1 mode is implemented in the frequency range 5.9 rad/s $\le \omega \le$ 6.3 rad/s. This zone contains, i.e. "captures", resonance. It is T-periodic regime with one direct impact per cycle on the primary structure and one impact on the obstacle rigidly connected to it.

Table 1

The dynamic behavior of the system with the damper of ***V3*** variant
at the different exciting force frequencies

ω , rad/s	5.2	5.3	5.4	5.9	6.5	6.6	6.7	7.1
$E_{1max,}$ J no damp	79.47	94.12	113.5	446.1	811.2	534.4	366.7	122.9
E_{1max},J for ***V3***	83.56	99.65	119.8	123.0	394.3	332.4	256.0	103.7
Regime for ***V3***	T,0,0	3T,1,0	2T,1,0	T,1,1	8T,6,4 (AM)	2T,1,0	3T,1,0	T,0,0

Fig. 7 shows its characteristics at ω =6.0 rad/s. This frequency corresponds to the larger resonance peak on the black curve in Fig. 6. The characteristics shown are typical for a periodic regime. In terms of orbital resonance, this regime can be called a 1:1 resonance because both bodies have the same period of oscillation.

ISSN 2410-2547
Опір матеріалів і теорія споруд/Strength of Materials and Theory of Structures. 2024. № 112

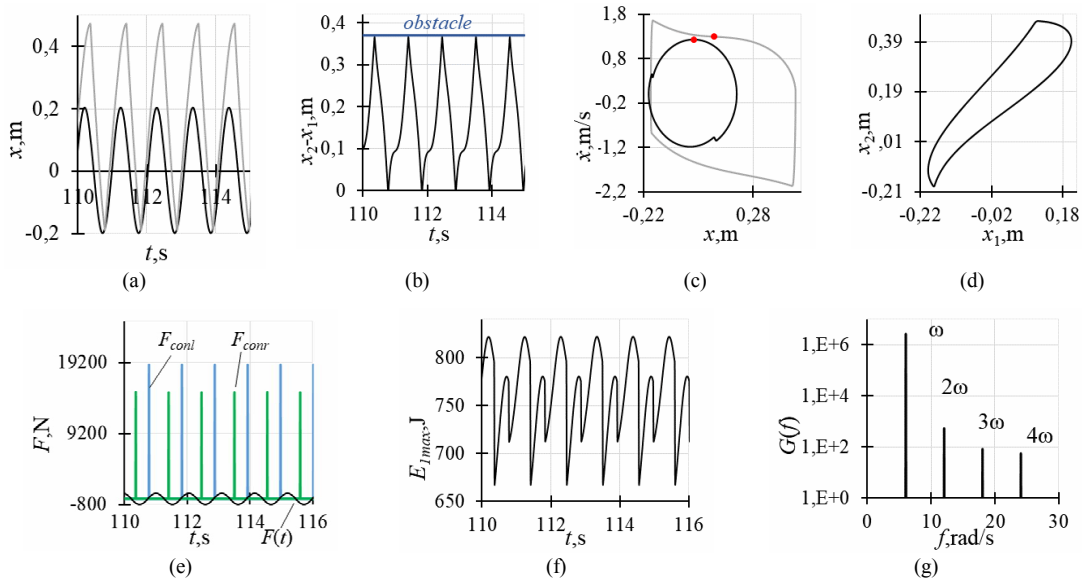

Fig. 7. Characteristics of T,1,1 regime for damper of ***V3*** variant at ω=6.0 rad/s. (a) Time series for both bodies displacements. (b) The relative damper displacements. (c) The phase trajectories with Poincaré maps in red for both bodies. (d) The relationship between the both bodies displacements. (e) Contact forces during damper impacts on the PS in blue and on the obstacle in green. (f) The total energy of the primary structure. (g) Fourier spectrum

Fig. 7 (a) demonstrates the impacts between bodies. Fig. 7 (b) demonstrates the impacts between bodies at $x_2 - x_1$=0, i.e. $x_2 = x_1$, and the damper impacts on the obstacle at $x_2 - x_1 = C$=0.36 m. The phase trajectories in Fig. 7 (c) are closed curves, Poincaré maps are individual points. The phase trajectory for the lightweight damper (gray curve) has two large velocity jumps during impacts on the PS and the obstacle. The phase trajectory for the heavy PS (black curve) also has two velocity jumps, but they are very small. Recall that the damper hits the PS directly and hits the obstacle rigidly connected to it. The Fourier spectrum in logarithmic scale in Fig. 7 (g) shows the fundamental frequency ωand superharmonics 2ω, 3ω, 4ω. The Figs. 7 (a), (b), (e), (f) clearly demonstrate the movement periodicity and the coincidence of the periods of both bodies motion. This gives reason to call this mode 1:1 resonance. Immediately after resonance at ω=6.4 and 6.5 rad/s, we observe an interesting 8T,6,4 mode. This is periodic regime of 8T period with 6 damper impacts on the PS and 4 impacts on the obstacle. This is amplitude-modulated regime. In many papers [38, 40, 41] this phenomenon is called strongly modulated response (SMR) and is discussed. It is sometimes referred to as weakly modulated response (WMR). There is no estimated numerical criterion for the depth of strong or weak modulation. In [42], the authors note that SMR "maybe rather ubiquitous in the forced system with essential nonlinearity and strong mass asymmetry. This type of response exists in a vicinity of exact 1:1 resonance". Indeed, we observe SMR precisely in such a case. So, let's look at it in detail (Fig. 8).

Fig. 8 (c) and 8 (j) demonstrate the existence of the 6 damper impacts against the primary structure directly at $x_2 - x_1$=0. Fig. 8 (c) and 8 (k) demonstrate the presence of the 4 damper impacts on an obstacle at $x_2 - x_1 = C$=0.36 m. Figs. 8 (j), (k), and (l) show the contact forces during these impacts. The Fourier spectrum in Fig. 8 (g), plotted on a logarithmic scale, shows the carrier frequency ω =6.5 rad/s and the subharmonics that are multiple of ω/8. The modulating frequency of the envelope Ω, shown in Fig.8 (a) in red, is 1/8 from the carrier frequency. The envelope is constructed using the Hilbert transform. Then the subharmonics in Fig. 8 (g) can be represented as ($\omega \pm n\Omega$) as shown in Fig. 8 (h). Fig. 8 (i) shows the Fourier spectrum of the modulating signal, i.e., of the envelope. In this spectrum, its fundamental frequency Ω and superharmonics $2\Omega, 3\Omega, 4\Omega$ can be seen. It is clearly seen that $\Omega = \omega/8 = 6.5/8$ rad/s=0.8125 rad/s.

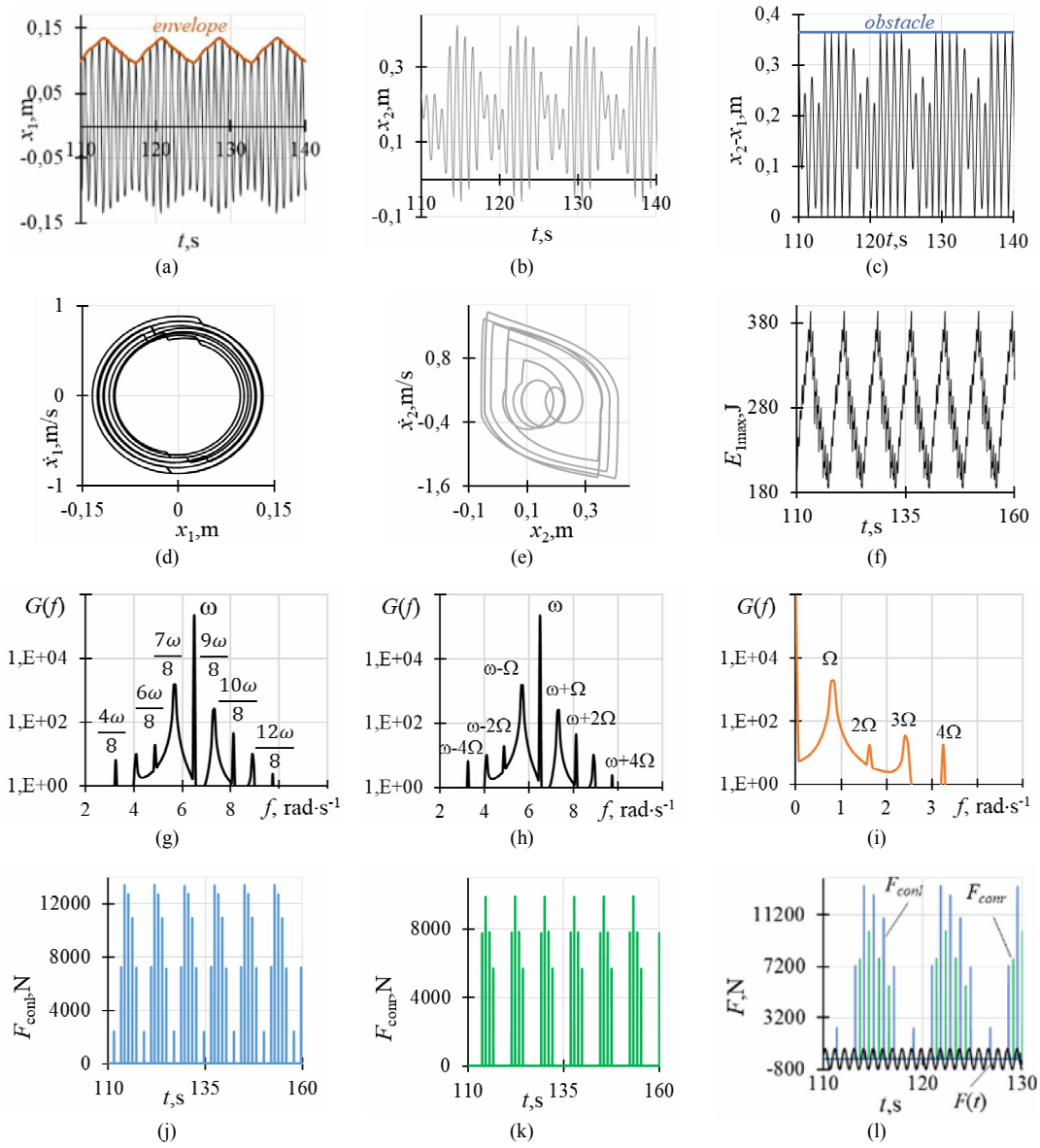

Fig. 8. Amplitude modulated signal for damper of ***V3*** variant at ω=6.5 rad/s

Then, in the frequency range 6.7 rad/s $\leq \omega \leq$ 7.0 rad/s, the periodic 3*T*,1.0 mode is realized again. At both edges of the frequency range, both on the left at low frequencies $\omega \leq$ 5.2 rad/s and on the right at high frequencies $\omega \leq$ 7.1 rad/s, the VI NES does not hit either the primary structure or the obstacle. Periodic shockless mode *T*,0,0 is implemented.

Thus, the MATLAB tools allowed us to find the optimal VI NES design. The damper of ***V3*** variant, which has such design, mitigates the primary structure vibrations quite well and strongly reduces its resonant peak. However, we must once again pay attention to two important details. Firstly, the damper operates as a nonlinear vibro-impact one in a fairly narrow range of the exciting force. This range covers the region near the resonant frequency. In the other frequency ranges, it works as a shockless linear damper. Secondly, the clearance in this optimal design is very large. This causes the damper to oscillate at some frequencies without impacts.

ISSN 2410-2547
Опір матеріалів і теорія споруд/Strength of Materials and Theory of Structures. 2024. № 112

5. Parameters optimization for damper with mass m_2=40 kg

5.1. Search of the optimal design

The mass of this damper is 4% of the primary structure mass. We have analyzed the operation of this damper with two different parameter sets. In the first option, we have used the parameters found for the damper of ***V3*** variant in Sec.4. We called it variant ***V4***.

V4: m_2=40 kg, k_2 = 215 N/m, c_2=232 N·s/m, C=0.36 m,

D= 0.06 m, E_2 =2.21·10^7 N/m^2, E_4 =2.05·10^7 N/m^2, $\nu_2 = \nu_4$=0.4.

We have carried out an optimization procedure to get another variant. The same tools as the previous ones helped to perform this procedure. We observed that increasing the clearance allows us to obtain a smaller value of the maximum total energy of the PS. The graph (D -C) in Fig.5 confirms this assumption. Therefore, it is advisable to construct it with new parameters and within new boundaries. Fig. 9 shows it. The MATLAB *fminsearch* program, although looking for local minima, showed that a large increase in the clearance value greatly reduces the maximum PS energy. At the same time, it showed a reduction in the damping coefficient. Therefore, we chose another variant of the damper parameters in this way:

V5: m_2=40 kg, k_2 = 215 N/m, c_2=64.1 N·s/m, C=0.673 m,

D= 0.03 m, E_2 =2.21·10^7 N/m^2, E_4 =2.05·10^7 N/m^2, $\nu_2 = \nu_4$=0.4.

In the next section, we show the performance of the dampers of ***V4*** and ***V5*** variants.

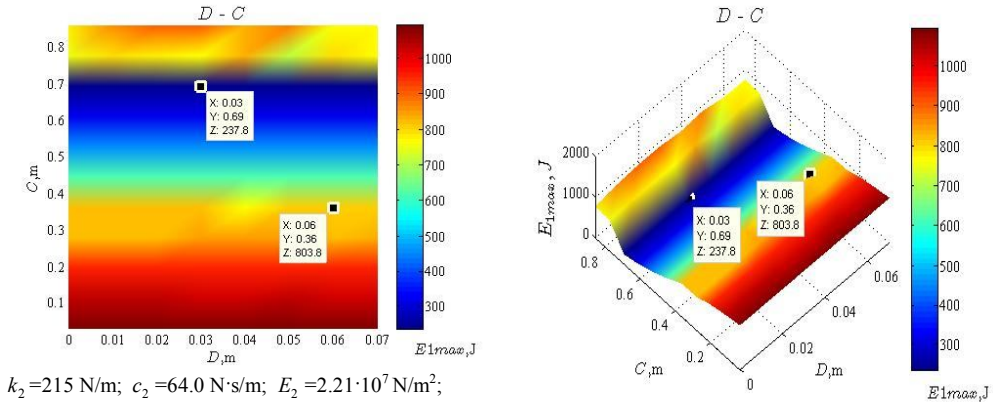

k_2 =215 N/m; c_2 =64.0 N·s/m; E_2 =2.21·10^7 N/m^2;

E_4 =2.05·10^7 N/m^2; $\nu_2 = \nu_4 = 0.4$

Fig. 9. The relationships between damper parameters D and C

5.2. Dynamic behavior of the primary structure coupled to the vibro-impact dampers of *V4* and *V5* variants

Fig.10 shows the maximum total energy of the primary structure depending on the exciting force frequency.

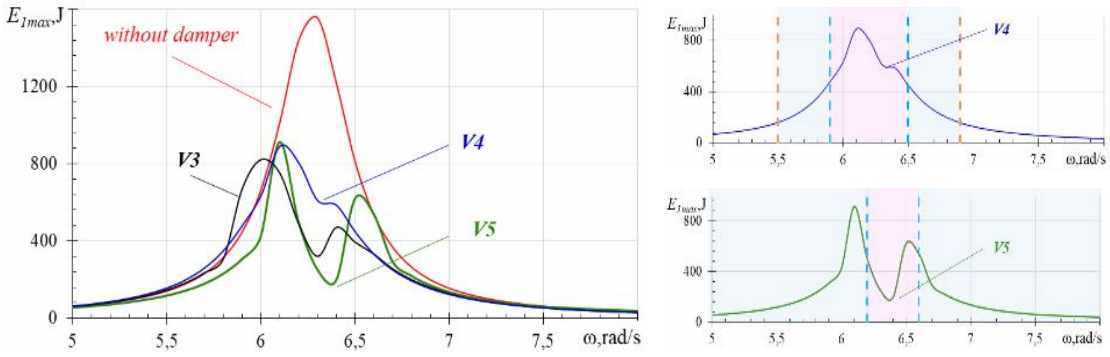

Fig. 10. Maximum total energy of the primary structure coupled to the dampers of ***V3***, ***V4***, ***V5*** variants

We clearly see the difference between the system behavior with dampers of the ***V4*** and ***V5*** variants, although both variants reduce the PS energy very much. Comparing them to the ***V3*** variant, one can see that their resonant peak is larger. But they do not increase the PS energy even at frequencies lower than the resonant one. Let us emphasize that the clearance in ***V5*** variant C -D = 0.643 m is huge one. Because of this, the impacts of a vibro-impact damper on the obstacle occur in very narrow region of the frequencies close to the resonant one. This narrow region of the damper impacts against both the PS directly and an obstacle is 5.9 rad/s $\le \omega \le$ 6.5 rad/s in ***V5*** variant. The blue dotted vertical lines in Fig. 10 mark it. It is colored pink. Impacts only against PS without impacts on an obstacle occur throughout the entire frequency range in ***V5*** variant. In variant ***V4***, they occur in the region, bounded by the brown dotted vertical lines. It is colored blue. Let us consider the effect of such a large clearance on the system dynamics in more detail. Table 2 shows the regime alternation when the exciting force frequency changes.

Table 2

The dynamic behavior of the system with the dampers of ***V4*** and ***V5*** variants at the different exciting force frequencies

ω, rad/s	5.3	5.5	6.0	6.1	6.4	6.5	6.9	7.0
E_{1max}, J no damp.	94.12	139.9	664.8	1015.3	1220	811.2	198	153.9
E_{1max}, J for ***V4***	104.2	157.1	634.8	889.8	585.3	447.5	153.5	124.2
Regime for ***V4***	T,0,0	**2*T*,1,0**	3T,2,1	T,1,1	Chaotic	2T,1,0	3T,1,0	T,0,0
E_{1max},J for ***V5***	82.35	116.4	422.6	912.8	194.1	618.5	169.9	135.4
Regime for ***V5***	T,1,0	T,1,0	**2*T*,2,0**	2T,1,0	T,1,1	8T,6,4 (AM)	2T,1,0	2T,1,0

It is interesting to compare two 2T-periodic regimes. Regime 2T,1,0 with one impact on the PS per cycle at $\omega = 5.5$ rad/s in ***V4*** variant and regime 2T,2,0 with two impacts on the PS per cycle at $\omega = 6.0$ rad/s in ***V5*** variant. There are no impacts on the obstacle in both modes.

Fig.11 shows the mode characteristics for ***V4*** and Fig. 12 for ***V5***.

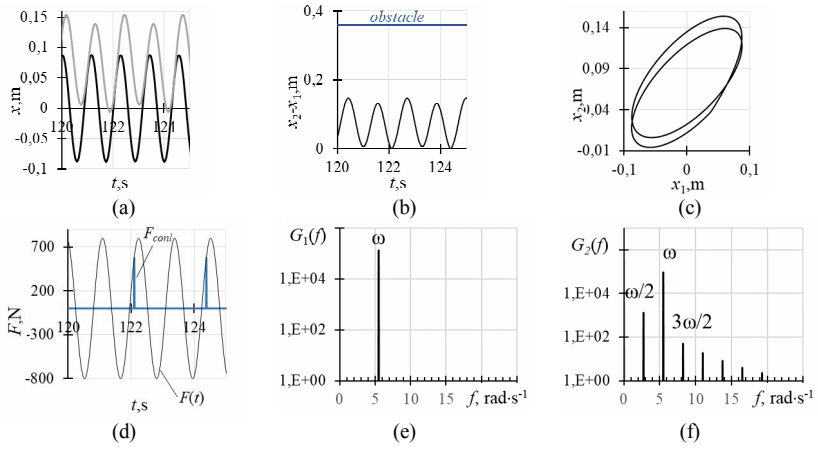

Fig. 11. Characteristics of the 2T-periodic movement 2T,1,0 of the damper of ***V4*** variant at the exciting force frequency $\omega = 5.5$ rad/s. (a) Time series of the both bodies displacements. (b) The relative damper displacement. (c) The relationship between the both bodies displacements. (d) Contact forces during damper impacts on the PS in blue. (e) Fourier spectrum for the PS. (g) Fourier spectrum for the damper

Fig. 11 (a) shows the sliding impact of the damper against the PS. Therefore, the contact force in Fig. 11 (d) is small, even less than the exciting force amplitude. Fig. 11 (b) shows how far away from the obstacle the damper oscillates. The Fourier spectrum in Fig. 11 (e) represents the fundamental frequency ω for the PS movement. The Fourier spectrum in Fig. 11 (f) represents the fundamental frequency ω and subharmonics $\omega/2$, $3\omega/2$ for the damper movement. In terms of orbital resonance, this mode can be called a 2:1 resonance. The damper cycle is twice the PS cycle. This means that the

ISSN 2410-2547
Опір матеріалів і теорія споруд/Strength of Materials and Theory of Structures. 2024. № 112

PS completes two of its cycle in the time it takes the damper to complete one cycle. Another movement picture is shown in Fig.12 for the 2*T*-periodic 2*T*,2,0 mode at ω=6.0 rad/s for ***V5*** variant.

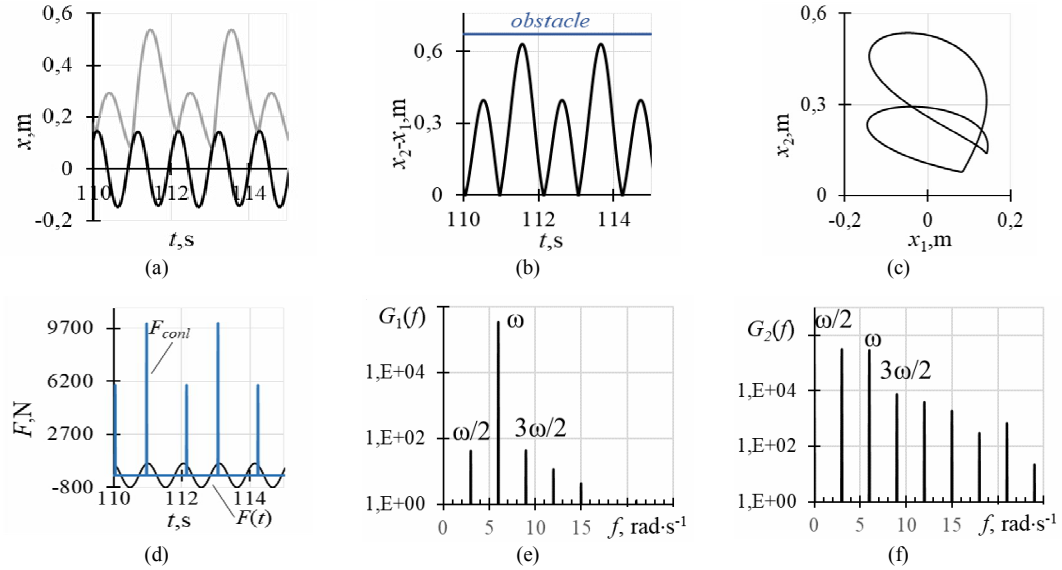

Fig. 12 Characteristics of the 2*T*-periodic movement 2*T*,2,0 of the damper of ***V5*** variant at the exciting force frequency ω =6.0 rad/s. (a) Time series of the both bodies displacements. (b) The relative damper displacement. (c) The relationship between the both bodies displacements. (d) Contact forces during damper impacts on the PS in blue. (e) Fourier spectrum for the PS. (g) Fourier spectrum for the damper

Fig. 12 (a) shows two impacts of the damper on the PS during oncoming traffic. Therefore, the contact force in Fig.12 (d) is large, much greater than the exciting force amplitude. Fig. 12 (b) shows how close to the obstacle the damper oscillates. The Fourier spectra in Fig. 12 (e) and Fig. 12 (f) represent the fundamental frequency ω and subharmonics $\omega/2$, $3\omega/2$ for both PS and damper movement. In terms of orbital resonance, this mode can be called a 1:1 resonance. The PS and the damper cycles are the same, although this cycle is equal to two periods of the exciting force. This means that the PS accomplishes its one cycle in the same amount of time it takes the damper to accomplish its one cycle.

Thus, the MATLAB tools allowed us to find the optimal VI NES design in this case as well. The dampers of ***V4*** and ***V5*** variants, which have such design, mitigates the primary structure vibrations quite well and strongly reduces its resonant peak. However, we must once again pay attention to two important details. Firstly, the damper operates as a nonlinear vibro-impact one in a fairly narrow range of the exciting force. This range covers the region near the resonant frequency. In the other frequency ranges, it works as a shockless linear damper. Secondly, the clearance in this optimal design is very large. This causes the damper to oscillate at some frequencies without impacts.

Comparing the operation of the dampers of ***V1*** and ***V2*** variants with the dampers of ***V3***,***V4*** and ***V5*** variants, one can clearly see that they differ significantly in both design and efficiency. This once again emphasizes that not only the sequence of the optimization procedure is ambiguous, but also its results. Therefore, the resulting damper designs need to be tested and carefully analyzed. We have shown what modes arise in the system when the primary structure is coupled to the different dampers at different exciting force frequencies.

6. Conclusions

The results presented in the above sections lead to the following conclusions.

1. This paper studies the optimization process of a 2-DOF vibro-impact system consisting of a heavy primary structure and a lightweight vibro-impact damper (VI NES). The optimization procedure involves searching for the optimal damper design that ensures its maximum efficiency.

2. The epigraph to this paper can be the quote we cited earlier: “There is no exact methodto simplify the design of the multiparameter nonlinear energy sinks” [13].
3. Taking into account the synergistic effect of multiple parameter optimization, it would be advisable to optimize all damper parameters simultaneously rather than sequentially. However, due to the lack of appropriate software, we optimized all damper parameters alternately in several steps, testing the effect from each step.
4. The optimization procedure is ambiguous and contains a sufficient amount of arbitrariness. It can find different sets of optimal damper design. Above we emphasized that there are many sets of parameter values that provide the objective function minimum. The authors of [6] wrote: “The nonlinear stiffness properties have significant influence on control effectiveness, and they can be implemented in numerous scenarios with plenty of configuration parameters.”
5. The MATLAB proposes several algorithms for finding the objective function minimum. We have used some of them. The programs fminsearch and fmincon, which find local minima of the objective function, yield different sets of the damper parameters that provide minimum values of the objective function in the chosen region. The genetic algorithm ga, which selects random intermediate results, yields randomly selected parameter sets from the optimal parameters manifold. We did not use this algorithm. The program surf allows us to construct parameter pair surfaces that show parameter ranges with corresponding objective function values.
6. Setting the objective function and its parameters plays a crucial role in the optimization process. Naturally, some of these parameters are precisely the ones to be optimized. We have chosen the maximum total energy of the primary structure coupled to the vibro-impact NES as the objective function.
7. We believe that it is reasonable to optimize the damper parameters separately for each selected damper mass.
8. Each chosen set of optimal damper parameters should be carefully tested and analyzed.
9. We compared the five obtained optimal designs for dampers with two different masses. When analyzing them, we observed different motion modes, namely periodic modes of different periodicity with different number of impacts, with different ratio of bodies motion periods: 1:1 resonance with resonance capture and 2:1 resonance; regime 8*T*,6,4 (SMR).
10. The single-sided VI NES with one obstacle practically works as double-sided VI NES, since it hits both the primary structure directly and the obstacle rigidly coupled to it. The primary structure in this case plays the role of a second constraint.
11. The impact simulation in accordance with Hertz’s contact law allows us: firstly, to include the mechanical characteristics of colliding surfaces in the list of optimizing parameters and, secondly, to calculate the contact impact forces during damper impacts both directly on the primary structure and on the obstacle.
12. The final decision on the optimal damper design may be made taking into account various engineering considerations regarding its mass and other parameters. It should be based on the options obtained as a result of the optimization procedure.

REFERENCES

1. Kumar R., Kuske R., Yurchenko D. Exploring effective TET through a vibro-impact nonlinear energy sink over broad parameter regimes //Journal of Sound and Vibration. – 2024. – T. 570. – C. 118131. https://doi.org/10.1016/j.jsv.2023.118131
2. Gendelman O. V. Transition of energy to a nonlinear localized mode in a highly asymmetric system of two oscillators Transition of Energy to a Nonlinear Localized Mode in a Highly Asymmetric System of Two Oscillators //Nonlinear dynamics. – 2001. – T. 25. – C. 237-253. https://doi.org/10.1007/978-94-017-2452-4_13
3. Vakakis A. F., Gendelman O. Energy pumping in nonlinear mechanical oscillators: part II– resonance capture //J. Appl. Mech. – 2001. – T. 68. – №. 1. – C. 42-48. https://doi.org/10.1115/1.1345525
4. Ding H., Chen L. Q. Designs, analysis, and applications of nonlinear energy sinks //Nonlinear Dynamics. – 2020. – T. 100. – №. 4. – C. 3061-3107. https://doi.org/10.1007/s11071-020-05724-1
5. Saeed A. S., Abdul Nasar R., AL-Shudeifat M. A. A review on nonlinear energy sinks: designs, analysis and applications of impact and rotary types //Nonlinear Dynamics. – 2023. – T. 111. – №. 1. – C. 1-37. https://doi.org/10.1007/s11071-022-08094-y
6. Lu Z. et al. Nonlinear dissipative devices in structural vibration control: A review //Journal of Sound and Vibration. – 2018. – T. 423. – C. 18-49.http://dx.doi.org/10.1016/j.jsv.2018.02.052

7. Lee Y. S. et al. Passive non-linear targeted energy transfer and its applications to vibration absorption: a review //Proceedings of the Institution of Mechanical Engineers, Part K: Journal of Multi-body Dynamics. – 2008. – Т. 222. – №. 2. – С. 77-134. http://dx.doi.org/10.1243/14644193jmbd118
8. Wierschem N. E. Targeted energy transfer using nonlinear energy sinks for the attenuation of transient loads on building structures. – University of Illinois at Urbana-Champaign, Newmark Structural Engineering Laboratory Report Series 045. 2014. https://www.ideals.illinois.edu/items/89701
9. Lu, Z., Wang, Z., Masri, S. F., & Lu, X. Particle impact dampers: Past, present, and future //Structural Control and Health Monitoring. – 2018. – Т. 25. – №. 1. – С. e2058.http://dx.doi.org/10.1002/stc.2058
10. Wang, J., Wierschem, N. E., Spencer Jr, B. F., & Lu, X. Track nonlinear energy sink for rapid response reduction in building structures //Journal of Engineering Mechanics. – 2015. – Т. 141. – №. 1. – С. 04014104. http://dx.doi.org/10.1061/(asce)em.1943-7889.0000824
11. Dekemele K., Habib G. Inverted resonance capture cascade: modal interactions of a nonlinear energy sink with softening stiffness //Nonlinear Dynamics. – 2023. – Т. 111. – №. 11. – С. 9839-9861. https://doi.org/10.1007/s11071-023-08423-9
12. Al-Shudeifat M. A., Saeed A. S. Periodic motion and frequency energy plots of dynamical systems coupled with piecewise nonlinear energy sink //Journal of Computational and Nonlinear Dynamics. – 2022. – Т. 17. – №. 4. – С. 041005. https://doi.org/10.1115/1.4053509
13. Kang, X., Tang, J., Xia, G., Wei, J., Zhang, F., & Sheng, Z.Design, Optimization, and Application of Nonlinear Energy Sink in Energy Harvesting Device //International Journal of Energy Research. – 2024. – Т. 2024. doi:10.1155/2024/2811428. 615 URL http://dx.doi.org/10.1155/2024/2811428
14. Al-Shudeifat, M. A., Wierschem, N., Quinn, D. D., Vakakis, A. F., Bergman, L. A., & Spencer Jr, B. F. Numerical and experimental investigation of a highly effective single-sided vibro-impact non-linear energy sink for shock mitigation //International journal of non-linear mechanics. – 2013. – Т. 52. – С. 96-109. https://doi.org/10.1016/j.ijnonlinmec.2013.02.004
15. Pennisi G. Passive vibration control by using Nonlinear Energy Sink absorbers. Theoretical study and experimental investigations :дис. – INSTITUT SUPERIEUR DE L'AERONAUTIQUE ET DE L'ESPACE (ISAE), 2016. https://hal.science/tel-01471929
16. Liu R., Kuske R., Yurchenko D. Maps unlock the full dynamics of targeted energy transfer via a vibro-impact nonlinear energy sink //Mechanical Systems and Signal Processing. – 2023. – Т. 191. – С. 110158. https://doi.org/10.1016/j.ymssp.2023.110158
17. Boroson E., Missoum S. Stochastic optimization of nonlinear energy sinks //Structural and Multidisciplinary Optimization. – 2017. – Т. 55. – С. 633-646. https://doi.org/10.1007/s00158-016-1526-y
18. Snoun C., Bergeot B., Berger S. Robust optimization of nonlinear energy sinks used for mitigation of friction-induced limit cycle oscillations //European Journal of Mechanics-A/Solids. – 2022. – Т. 93. – С. 104529. https://doi.org/10.1016/j.euromechsol.2022.104529
19. Theurich T., Krack M. Experimental validation of impact energy scattering as concept for mitigating resonant vibrations //Journal of Structural Dynamics. – 2023. – Т. 2. – С. 1-23.https://doi.org/10.25518/2684-6500.126
20. Costa D., Kuske R., Yurchenko D. Qualitative changes in bifurcation structure for soft vs hard impact models of a vibro-impact energy harvester //Chaos: An Interdisciplinary Journal of Nonlinear Science. – 2022. – Т. 32. – №. 10. https://doi.org/10.1063/5.0101050
21. Feudo, S. L., Job, S., Cavallo, M., Fraddosio, A., Piccioni, M. D., &Tafuni, A. Finite contact duration modeling of a Vibro-Impact Nonlinear Energy Sink to protect a civil engineering frame structure against seismic events //Engineering Structures. – 2022. – Т. 259. – С. 114137. https://doi.org/10.1016/j.engstruct.2022.114137
22. Okolewski A., Blazejczyk-Okolewska B. Hard vs soft impacts in oscillatory systems' modeling revisited //Chaos: An Interdisciplinary Journal of Nonlinear Science. – 2021. – Т. 31. – №. 8. https://doi.org/10.1063/5.0057029
23. Blazejczyk-Okolewska B., Czolczynski K., Kapitaniak T. Classification principles of types of mechanical systems with impacts–fundamental assumptions and rules //European Journal of Mechanics-A/Solids. – 2004. – Т. 23. – №. 3. – С. 517-537. https://doi.org/10.1016/j.euromechsol.2004.02.005
24. Andreaus U., Chiaia B., Placidi L. Soft-impact dynamics of deformable bodies //Continuum Mechanics and Thermodynamics. – 2013. – Т. 25. – С. 375-398. https://doi.org/10.1007/s00161-012-0266-5
25. Bazhenov V. A., Pogorelova O. S., Postnikova T. G. Comparison of two impact simulation methods used for nonlinear vibroimpact systems with rigid and soft impacts //Journal of Nonlinear Dynamics. – 2013. – Т. 2013. https://doi.org/10.1155/2013/485676
26. Bazhenov V., Pogorelova O., Postnikova T. Crisis-induced intermittency and other nonlinear dynamics phenomena in vibro-impact system with soft impact //Nonlinear Mechanics of Complex Structures: From Theory to Engineering Applications. – 2021. – С. 185-203. https://doi.org/10.1155/2013/485676
27. Goldsmith W. Impact: the Theory and Physical Behavior of Colliding Solids, Edward Arnold Ltd //London, England. – 1960.
28. Johnson K. L. Contact mechanics. – Cambridge university press, 1987.
29. Lizunov P., Pogorelova O., Postnikova T. The synergistic effect of the multiple parameters of vibro-impact nonlinear energy sink //Journal of AppliedMath. – 2023. – Т. 1. – №. 3. https://doi.org/10.59400/jam.v1i3.199
30. Lizunov P. P., Pogorelova O., Postnikova T. Vibro-impact damper dynamics depending on system parameters. – 2023. Research Square. https://doi.org/10.21203/rs.3.rs-2786639/v1
31. Lizunov P., Pogorelova O., Postnikova T. Selection of the optimal design for a vibro-impact nonlinear energy sink //Strength of Materials and Theory of Structures. – 2023. – №. 111. – С. 13-24.https://doi.org/10.32347/2410-2547.2023.111.13-24
32. Al-Shudeifat, M. A., Wierschem, N., Quinn, D. D., Vakakis, A. F., Bergman, L. A., & Spencer Jr, B. F. Numerical and experimental investigation of a highly effective single-sided vibro-impact non-linear energy sink for shock mitigation

//International journal of non-linear mechanics. – 2013. – Т. 52. – С. 96-109. https://www.sciencedirect.com/science/article/pii/ S0020746213000322
33. Lizunov P., Pogorelova O., Postnikova T. The Influence of Various Optimization Procedures on the Dynamics and Efficiency of Nonlinear Energy Sink with Synergistic Effect Consideration //Available at SSRN 4663138.https://doi.org/10.2139/ssrn.4663138
34. Saeed, A. S., AL-Shudeifat, M. A., Cantwell, W. J., &Vakakis, A. F. Two-dimensional nonlinear energy sink for effective passive seismic mitigation //Communications in Nonlinear Science and Numerical Simulation. – 2021. – Т. 99. – С. 105787. https://www.sciencedirect.com/science/article/pii/ S1007570421000988
35. Youssef B., Leine R. I. A complete set of design rules for a vibro-impact NES based on a multiple scales approximation of a nonlinear mode //Journal of Sound and Vibration. – 2021. – Т. 501. – С. 116043. https://doi.org/10.1016/j.jsv.2021.116043
36. AL-Shudeifat M. A., Saeed A. S. Comparison of a modified vibro-impact nonlinear energy sink with other kinds of NESs //Meccanica. – 2021. – Т. 56. – С. 735-752. https://doi.org/10.1007/s11012-020-01193-3
37. Javidialesaadi A., Wierschem N. E. Optimal design of rotational inertial double tuned mass dampers under random excitation //Engineering Structures. – 2018. – Т. 165. – С. 412-421. https://doi.org/10.1016/j.engstruct.2018.03.033
38. Li T. Study of nonlinear targeted energy transfer by vibro-impact :дис. – Toulouse, INSA, 2016. https://doi.org/10.1007/s11071-016-3127-0
39. Gourdon, E., Alexander, N. A., Taylor, C. A., Lamarque, C. H., & Pernot, S. Nonlinear energy pumping under transient forcing with strongly nonlinear coupling: Theoretical and experimental results //Journal of sound and vibration. – 2007. – Т. 300. – №. 3-5. – С. 522-551. https://doi.org/10.1016/j.jsv.2006.06.074
40. Gendelman O. V. Targeted energy transfer in systems with external and self-excitation //Proceedings of the Institution of Mechanical Engineers, Part C: Journal of Mechanical Engineering Science. – 2011. – Т. 225. – №. 9. – С. 2007-2043. https://doi.org/10.1177/0954406211413976
41. Gendelman O. V., Alloni A. Forced system with vibro-impact energy sink: chaotic strongly modulated responses //Procedia IUTAM. – 2016. – Т. 19. – С. 53-64. https://doi.org/10.1016/j.piutam.2016.03.009
42. Starosvetsky Y., Gendelman O. V. Strongly modulated response in forced 2DOF oscillatory system with essential mass and potential asymmetry //Physica D: Nonlinear Phenomena. – 2008. – Т. 237. – №. 13. – С. 1719-1733. https://doi.org/10.1016/j.physd.2008.01.019

Стаття надійшла 26.03.2024

Лізунов П.П., Погорелова О.С., Постнікова Т.Г.

ОПТИМІЗАЦІЯ КОНСТРУКЦІЇ ВІБРОУДАРНОГО ДЕМПФЕРА ЗА ДОПОМОГОЮ ІНСТРУМЕНТАРІЮ MATLAB

У роботі досліджено динаміку віброударної системи, що складається з основної (первинної) конструкції та сполученого з нею віброударного демпфера. Віброударний демпфер це віброударний нелінійний поглинач енергії (VINES). Оптимальна конструкція демпфера повинна забезпечувати найкраще пом'якшення вібрації основної конструкції. Процедури оптимізації для пошуку оптимального дизайну NES виконуються за допомогою стандартних засобів MATLAB. Ми використовували різні програми MATLAB, а саме програму *surf*, яка графічно показує діапазони пар параметрів, які потрібно оптимізувати; програми *fminsearch* і *fmincon*, які шукають локальні мінімуми цільової функції. Показано, що сама процедура оптимізації неоднозначна і містить достатню довільність. Її результат теж неоднозначний тому, що існує багато можливих наборів параметрів демпфера, які можуть забезпечити максимальне пом'якшення вібрацій основної конструкції. Ми не використовуємо генетичний алгоритм *ga*, оскільки він вибирає випадкові проміжні результати та дає випадково вибрані набори параметрів із різноманітності оптимальних параметрів. Встановлення цільової функції та її параметрів відіграє вирішальну роль у процесі оптимізації. За цільову функцію ми обрали максимальну повну енергію первинної структури. Кожен отриманий варіант набору параметрів демпфера повинен бути ретельно перевірений і проаналізований.Було порівняне п'ять отриманих оптимальних конструкцій демпфера з двома різними масами. При їхньому аналізі ми спостерігали різні режими руху, а саме періодичні режими різної періодичності з різною кількістю ударів за цикл, з різним співвідношенням періодів руху тіл: резонанс 1:1 із захопленням резонансу та резонанс 2:1; багато періодичний режим із багатьма ударами за цикл, якій виявивсяамплітудно-модульованим режимом. Остаточне рішення щодо оптимальної конструкції демпфера може бути прийнято з урахуванням різних інженерних міркувань щодо його маси та інших параметрів. Воно має базуватися на варіантах, отриманих в результаті процедури оптимізації.

Ключові слова: оптимізація, демпфер, набір параметрів, віброудар, нелінійний поглинач енергії.

Lizunov P.P., Pogorelova O.S., Postnikova T.G.

OPTIMIZATION OF A VIBRO-IMPACT DAMPER DESIGN USING MATLAB TOOLS

The paper studies the dynamics of a vibro-impact system consisting of a main (primary) structure and a vibro-impact damper coupled to it. A vibro-impact damper is a vibro-impact nonlinear energy sink (VI NES). The optimal damper design should provide the best vibration mitigation for the primary structure. The optimization procedures for finding the optimal NES design are carried out using standard MATLAB tools. We used different MATLAB programs, namely *surf* program, which graphically shows the ranges of parameter pairs to be optimized; *fminsearch* and *fmincon*programs, which search for local minima of the objective function. It is shown that the optimization procedure itself is ambiguous and contains a sufficient amount of arbitrariness. Its result is also ambiguous. It is due to the presence of the many possible sets of damper parameters that can provide maximum mitigation of the main structure vibrations. We do not use the genetic algorithm *ga*because it selects random intermediate results and yields randomly selected parameter sets from the optimal parameters manifold. Setting the objective function and its parameters plays a crucial role in the optimization process. We have chosen the maximum total energy of the primary structure as the objective function. Each resulting variant of the damper parameter set should be carefully tested and

analyzed. We compared the five obtained optimal designs for dampers with two different masses. When analyzing them, we observed different motion modes, namely periodic modes of different periodicity with different number of impacts per cycle, with different ratio of bodies motion periods: 1:1 resonance with resonance capture and 2:1 resonance; amulti-periodic mode with many impacts per cycle, which turned out to be an amplitude-modulated mode – Amplitude Modulated Signal . The final decision on the optimal damper design may be made taking into account various engineering considerations regarding its mass and other parameters. It should be based on the options obtained as a result of the optimization procedure.

Keywords: optimization, damper, parameter set, vibro-impact, nonlinear energy sink.

UDC 539.3
Lizunov P.P., Pogorelova O.S., Postnikova T.G. **Optimization of a vibro-impact damper design using MATLAB tools** //Strength of Materials and Theory of Structures: Scientific-and-technical collected articles. – K.: KNUBA. 2024. – Issue 112. – P. 3-18.
The paper studies the dynamics of a vibro-impact system consisting of a main (primary) structure and a vibro-impact nonlinear energy sink (VI NES) coupled to it. The optimization procedures for finding the optimal NES design are carried out using standard MATLAB tools. The ambiguity of the optimization results is shown. It is due to the presence of the many possible sets of damper parameters that can provide maximum mitigation of the main structure vibrations. Each resulting variant of the damper parameter set is tested and analyzed. Comparison the results of analyzing different options should help to select the final optimal damper design. By analyzing the motion of the system with different damper variants, we observed various periodic oscillatory modes, namely 1:1 resonance, 2:1 resonance, and strongly modulated response.
Tabl. 2. Fig. 12. Ref. 42.

УДК 539.3
Лізунов П.П., Погорелова О.С., Постнікова Т.Г. **Оптимізація конструкції віброударного демпфера за допомогою інструментарію MATLAB** // Опірматеріалів і теоріяспоруд: наук.-тех. збірн. – К.: КНУБА. 2024. – Вип. 112. – С. 3-18. – Англ.
Досліджено динаміку віброударної системи, що складається з основної (первинної) конструкції та з'єднаного з нею віброударного нелінійного поглинача енергії (VI NES). Оптимізаційні процедури для знаходження оптимальної конструкції NES виконано з використанням стандартного інструментарію MATLAB. Показано неоднозначність результатів оптимізації. Це пов'язано з наявністю багатьох можливих наборів параметрів демпфера, які можуть забезпечити максимальне гасіння коливань основної конструкції. Кожен отриманий варіант набору параметрів демпфера протестоване та проаналізоване. Порівняння результатів аналізу різних варіантів має допомогти вибрати остаточну оптимальну конструкцію демпфера. Аналізуючи рух системи з різними варіантами демпферів, ми спостерігали різні періодичні коливальні режими, а саме: резонанс 1:1, резонанс 2:1 та сильно модульований відгук.
Табл. 2. Рис. 12. Бібліогр. 42 назв.

Автор (науковий ступінь, вчене звання, посада): доктор технічних наук, професор, завідувач кафедри будівельної механіки КНУБА, директор НДІ будівельної механіки ЛІЗУНОВ Петро Петрович
Адреса робоча: 03680 Україна, м. Київ, проспект Повітряних Сил 31, Київський національний університет будівництва і архітектури
Робочий тел.: +38(044) 245-48-29
Мобільний тел.: +38(067)921-70-05
E-mail: lizunov@knuba.edu.ua
ORCIDID: http://orcid.org/0000-0003-2924-3025

Автор (науковий ступінь, вчене звання, посада): кандидат фізико-математичних наук, старший науковий співробітник, провідний науковий співробітник НДІ будівельної механіки ПОГОРЕЛОВА Ольга Семенівна
Адреса робоча: 03680 Україна, м. Київ, проспект Повітряних Сил 31, Київський національний університет будівництва і архітектури
Робочий тел.: +38(044) 245-48-29
Мобільний тел.: +38(067) 606-03-00
E-mail: pogos13@ukr.net
ORCID ID: http://orcid.org/0000-0002-5522-3995

Автор (науковий ступінь, вчене звання, посада): кандидат технічних наук, старший науковий співробітник, старший науковий співробітник НДІ будівельної механіки ПОСТНІКОВА Тетяна Георгіївна
Адреса робоча: 03680 Україна, м. Київ, проспект Повітряних Сил 31, Київський національний університет будівництва і архітектури
Робочий тел.: +38(044) 245-48-29
Мобільний тел.: +38(050) 353-47-19
E-mail: postnikova.tg@knuba.edu.ua
ORCID ID: https://orcid.org/0000-0002-6677-4127